SUBSPACE IDENTIFICATION OF PERIODICALLY SWITCHING HAMMERSTEIN-WIENER MODELS FOR MAGNETOSPHERIC DYNAMICS [1]

Harish J. Palanthandalam-Madapusi [*]
Dennis S. Bernstein [*] **Aaron J. Ridley** [**]

[*] *Department of Aerospace Engineering, University of Michigan, Ann Arbor, MI 48109-2140, USA.*
{hpalanth,dsbaero}@umich.edu
[**] *Department of Atmospheric, Oceanic, and Space Science, University of Michigan, Ann Arbor, MI 48109, USA. ridley@umich.edu*

Abstract: Two existing Hammerstein-Wiener identification algorithms and a third novel Hammerstein-Wiener identification algorithm are considered for application to the magnetospheric system. A modified subspace algorithm that allows missing data points is described and used for identifying periodically switching Hammerstein-Wiener models, to capture the periodically time-varying nature of the system. These models are used to predict ground-based magnetometer response using the ACE satellite measurements.

Keywords: System identification, Identification algorithms, Modelling, Models, Prediction, Space.

1. INTRODUCTION

The magnetosphere is the region of space dominated by the magnetic field of the Earth. By predicting magnetospheric conditions, damage to critical systems aboard satellites and large power transformers on the earth can be avoided. Although large-scale, first principles models of the magnetosphere exist (Powell *et al.*, 1999), they are extremely expensive to run in real-time, and have to be run at a poor resolution for real-time performance. While empirical models are simplistic compared to first principles models, they are useful for predicting specific quantities at specific locations.

Previous empirical models include neural network models (Weigel *et al.*, 2003) and Hammerstein-Wiener (H-W) models (Palanthandalam-Madapusi *et al.*, 2005), where the H-W model structure consists of linear dynamics with static input and output nonlinearities as shown in Figure 1. Since

measurements of magnetospheric conditions are made by ground-based magnetometers, which rotate with a one-day periodicity with respect to the magnetosphere, the system has a one-day periodicity. In (Palanthandalam-Madapusi *et al.*, 2005), a sinusoid is used as an additional input to emulate the periodically time-varying nature of the system. In the current work, periodically switching models are used to model the periodically time-varying nature of the system.

Fig. 1. Hammerstein-Wiener Model

In this paper, subspace-based identification methods for periodically switching H-W models of the magnetospheric system are considered. For this application, two existing H-W identification methods (Goethals *et al.*, 2004; Palanthandalam-Madapusi *et al.*, 2005) are used, and a third H-W identification algorithm is developed. These three algorithms are then used as the basis for identifying periodically switching H-W models.

Subspace identification for periodic systems is developed in (Hench, 1995; Verhaegen and Yu, 1995). In particular, (Hench, 1995) uses lifting to express the periodically time-varying identification problem as a set of linear time-invariant identification problems. However, for a slowly time-varying periodic system with a large period p, both these methods are inefficient, since they require the calculation and storage of p state space matrices. For example, in the magnetospheric system, which has a one-day periodicity with measurements at every minute, 1440 sets of state-space matrices have to be calculated and stored. Another issue with real-life data such as the magnetospheric data is that there are often missing data points.

To deal with these issues, first a subspace algorithm that allows for missing data points is described. Although this modification is known, it is of great practical importance and is apparently unpublished. Furthermore, this subspace algorithm is essential for identifying periodically switching models. This technique is used with the three H-W identification algorithms mentioned above to identify periodically switching H-W models for the magnetospheric system. With the focus on prediction, all three methods are compared and the results reported.

2. MAGNETOSPHERIC APPLICATION

Much of the dynamics in the magnetosphere is controlled by the Sun's atmosphere, which flows supersonically away from the Sun past the Earth and the other planets. The solar wind carries embedded in it the Sun's magnetic field, commonly referred to as the interplanetary magnetic field (IMF).

The solar wind and IMF interact with the magnetosphere producing phenomena such as the aurora and ionospheric currents. When the aurora and ionospheric currents become severe, the upper atmosphere can heat up dramatically and expand, causing increased drag on satellites. In addition, large ionospheric currents can drive currents in power lines, which can overwhelm, and destroy transformers. It is therefore important that we understand when and where these large currents may occur and be able to predict them.

The ACE satellite, which is positioned at the Lagrangian gravitational null point between the Sun and the Earth, measures the solar wind and IMF conditions approximately one hour before they encounter the magnetosphere. The exact delay is calculated based on the solar wind velocity. This delay implies that measurements made by the ACE satellite at time t, reach the Earth at approximately time $t + 1$ hour. Thus, the ACE measurements are delayed by roughly an hour for use as the inputs to the identified model. Most importantly, because of this delay, the identified model has a one-hour predictive capability since the inputs are available one hour into the future.

The goal of the current study is to use the ACE measurements to predict the magnetosphere conditions. The ionospheric currents cause magnetic perturbations that are measured by ground-based magnetometers. Thus, the magnetometer data can be used as an indication of the magnetospheric conditions. By predicting ground-based magnetometer response using the ACE data, one can determine possible disturbances and may be able to take steps to minimize damage.

3. HAMMERSTEIN-WIENER IDENTIFICATION

Three H-W identification algorithms are considered here. Based on these three algorithms, periodically switching H-W models are constructed in subsequent sections for the magnetospheric system.

The first method (Palanthandalam-Madapusi *et al.*, 2005) consists of a two step procedure, in which the Hammerstein subsystem is identified in the first step and the Wiener nonlinearity is identified as a second least-squares step. To identify the Hammerstein subsystem, a basis function expansion of the known inputs is used.

The second method also consists of a two step procedure. To identify the Hammerstein subsystem in the first step, the algorithm described in (Goethals *et al.*, 2004) is used, which uses least squares support vector machines. The step for identifying the Wiener nonlinearity is the same.

Due to lack of space, the reader is referred to (Palanthandalam-Madapusi *et al.*, 2005) and (Goethals *et al.*, 2004) for details of the first two H-W identification algorithms. The third method, which is a novel one-step H-W identification algorithm, is explained in detail in the next subsection.

3.1 One Step Hammerstein-Wiener Identification

Consider a Wiener system of the form
$$x_{k+1} = Ax_k + Bu_k, \qquad (3.1)$$
$$y_k = Cx_k + Gh(x_k) + Du_k, \qquad (3.2)$$

where $x \in \mathbb{R}^n$, $u \in \mathbb{R}^m$, $y \in \mathbb{R}^l$, $h : \mathbb{R}^n \to \mathbb{R}^q$, $A \in \mathbb{R}^{n \times n}$, $B \in \mathbb{R}^{n \times m}$, $C \in \mathbb{R}^{l \times n}$, $D \in \mathbb{R}^{l \times m}$ and $G \in \mathbb{R}^{l \times q}$. The linear part of the output equation is Cx_k, while $Gh(x)$ is the nonlinear part of the output equation.

3.1.1. Notation Define the output block Hankel matrices

$$Y_{0|2i-1} \triangleq \begin{bmatrix} y_0 & y_1 & \cdots & y_{j-1} \\ \vdots & \vdots & \ddots & \vdots \\ y_{i-1} & y_i & \cdots & y_{i+j-2} \\ \hline y_i & y_{i+1} & \cdots & y_{i+j-1} \\ \vdots & \vdots & \ddots & \vdots \\ y_{2i-1} & y_{2i} & \cdots & y_{2i+j-2} \end{bmatrix} \quad (3.3)$$

$$= \begin{bmatrix} Y_{0|i-1} \\ \hline Y_{i|2i-1} \end{bmatrix} = \begin{bmatrix} Y_p \\ \hline Y_f \end{bmatrix}, \quad (3.4)$$

where i and j are user-defined integers such that $i \geq n$ and $j \gg i$. Also,

$$Y_{0|2i-1} = \begin{bmatrix} Y_{0|i} \\ \hline Y_{i+1|2i-1} \end{bmatrix} = \begin{bmatrix} Y_p^+ \\ \hline Y_f^- \end{bmatrix}. \quad (3.5)$$

The subscript p denotes the 'past' and the subscript f denotes 'future'. The input block Hankel matrices $U_{0|2i-1}$, U_p, U_f, U_p^+ and U_f^- are defined as in (3.3)-(3.5) with y replaced by u. The definitions of the "nonlinear" block Hankel matrices $H_{0|2i-1}$, H_p, H_f, H_p^+ and H_f^- are analogous to (3.3)-(3.5) with y replaced by $h(x)$. The extended observability matrix is

$$\Gamma_i \triangleq \begin{bmatrix} C \\ CA \\ \vdots \\ CA^{i-1} \end{bmatrix}. \quad (3.6)$$

Since $i \geq n$, if (A, C) is observable, then Γ_i has rank n. Let $M_i \in \mathbb{R}^{li \times mi}$ be the lower block triangular Toeplitz matrix

$$M_i = \begin{bmatrix} D & 0 & 0 & \cdots & 0 \\ CB & D & 0 & \cdots & 0 \\ CAB & CB & D & \cdots & 0 \\ \vdots & \vdots & \vdots & \ddots & \vdots \\ CA^{i-2}B & CA^{i-3}B & \cdots & \cdots & D \end{bmatrix}, \quad (3.7)$$

and define $\Psi_i \in \mathbb{R}^{li \times qi}$ as

$$\Psi_i = \begin{bmatrix} G & \cdots & 0 \\ \vdots & \ddots & \vdots \\ 0 & \cdots & G \end{bmatrix}. \quad (3.8)$$

Finally, the state sequence $X_i \in \mathbb{R}^{n \times j}$ is

$$X_i \triangleq \begin{bmatrix} x_i & x_{i+1} & \cdots & x_{i+j-2} & x_{i+j-1} \end{bmatrix}. \quad (3.9)$$

3.1.2. State Estimation

Definition 1. The nonlinear system (3.1)-(3.2) is *observable* if the triple (A, C, G) is such that $\Theta_i \triangleq \begin{bmatrix} \Gamma_i & \Psi_i \end{bmatrix} \in \mathbb{R}^{li \times (n+qi)}$ has full column rank for all $i \geq n$.

Note that, for a system to be observable it is necessary that $li \geq n + qi$ for all $i \geq n$, which implies $l > q$. Also, a necessary condition for observability is that the pair (A, C) be observable in the linear sense.

Lemma 3.1. If the nonlinear system (3.1)-(3.2) is observable, then the intersection of the row space of the 'past' block Hankel matrix $W_p \triangleq \begin{bmatrix} U_p \\ Y_p \end{bmatrix}$ and row space of the 'future' block Hankel matrix $W_f \triangleq \begin{bmatrix} U_f \\ Y_f \end{bmatrix}$ contains the state sequence X_i.

Proof: From (3.1) and (3.2),

$$Y_p = \Gamma_i X_0 + \Psi_i H_p + M_i U_p, \quad (3.10)$$

$$Y_f = \Gamma_i X_i + \Psi_i H_f + M_i U_f. \quad (3.11)$$

Since the system is observable, (3.11) can be written as

$$\begin{bmatrix} X_i \\ H_f \end{bmatrix} = \begin{bmatrix} -\Theta_i^\dagger M_i & \Theta_i^\dagger \end{bmatrix} \begin{bmatrix} U_f \\ Y_f \end{bmatrix}, \quad (3.12)$$

where $\dagger$ is the Moore-Penrose generalized inverse. Furthermore,

$$X_i = \begin{bmatrix} -\Theta_{i,n}^\dagger M_i & \Theta_{i,n}^\dagger \end{bmatrix} \begin{bmatrix} U_f \\ Y_f \end{bmatrix}, \quad (3.13)$$

where $\Theta_{i,n}^\dagger$ denotes the first n rows of $\Theta_i^\dagger$. From (3.13), it is clear that the state sequence X_i is contained in the row space of W_f or the 'future' input-output data. Similarly from (3.10),

$$X_0 = \begin{bmatrix} -\Theta_{i,n}^\dagger M_i & \Theta_{i,n}^\dagger \end{bmatrix} \begin{bmatrix} U_p \\ Y_p \end{bmatrix}. \quad (3.14)$$

Next, X_0 and X_i are related as

$$X_i = A^i X_0 + \Delta_i U_p, \quad (3.15)$$

where

$$\Delta_i \triangleq \begin{bmatrix} A^{i-1}B & A^{i-2}B & \cdots & B \end{bmatrix}. \quad (3.16)$$

Now, using (3.14) and (3.15), we obtain

$$X_i = \begin{bmatrix} -A^i \Theta_{i,n}^\dagger M_i + \Delta_i & A^i \Theta_{i,n}^\dagger \end{bmatrix} \begin{bmatrix} U_p \\ Y_p \end{bmatrix}. (3.17)$$

From (3.17), the state sequence X_i is equally contained in the 'past' input-output data W_p. Thus from (3.13) and (3.17), the state sequence X_i is contained in the intersection of W_p and W_f. $\square$

Next, the notion of persistent excitation is defined.

Definition 2. A sequence of inputs $\{u_i\}_{i=1}^N$ is *persistently exciting* for the system (3.1)-(3.2) if the following conditions are satisfied:

(1) The matrix $\begin{bmatrix} H_{0|2i-1} \\ U_{0|2i-1} \end{bmatrix}$ has full row rank

(2) The intersection between the row space of the state sequence X_0 and row space of the matrix $\begin{bmatrix} H_{0|2i-1} \\ U_{0|2i-1} \end{bmatrix}$ is trivial

(3) The state sequence X_0 has full row rank n.

Theorem 3.1. If the nonlinear system (3.1) and (3.2) is observable and the input sequence $\{u_i\}_{i=1}^N$ is persistently exciting, then the intersection of the row spaces of the matrices W_p and W_f yields the state sequence X_i.

Proof. From Lemma 3.1, the intersection of W_p and W_f contains the state sequence X_i. Next, using (3.10), we write

$$\begin{bmatrix} Y_p \\ U_p \end{bmatrix} = \begin{bmatrix} \Gamma_i & \Psi_i & M_i \\ 0 & 0 & I_{mi} \end{bmatrix} \begin{bmatrix} X_0 \\ H_p \\ U_p \end{bmatrix}, \qquad (3.18)$$

which implies that

$$\text{rank} \begin{bmatrix} Y_p \\ U_p \end{bmatrix} = \text{rank} \begin{bmatrix} X_0 \\ H_p \\ U_p \end{bmatrix} = n + qi + mi.$$

Similarly, it can be shown that

$$\text{rank} \begin{bmatrix} Y_f \\ U_f \end{bmatrix} = \text{rank} \begin{bmatrix} X_i \\ H_f \\ U_f \end{bmatrix} = n + qi + mi$$

and

$$\text{rank} \begin{bmatrix} U_p \\ Y_p \\ U_f \\ Y_f \end{bmatrix} = \text{rank} \begin{bmatrix} X_0 \\ H_{0|2i-1} \\ U_{0|2i-1} \end{bmatrix} = n + 2qi + 2mi.$$

Now, using the Grassmann dimension theorem ((Bernstein, 2005), Theorem 2.3.1) gives

$$\dim \left(\text{row space} \begin{bmatrix} U_p \\ Y_p \end{bmatrix} \bigcap \text{row space} \begin{bmatrix} U_f \\ Y_f \end{bmatrix} \right)$$

$$= \text{rank} \begin{bmatrix} U_p \\ Y_p \end{bmatrix} + \text{rank} \begin{bmatrix} U_f \\ Y_f \end{bmatrix} - \text{rank} \begin{bmatrix} U_p \\ Y_p \\ U_f \\ Y_f \end{bmatrix}$$

$$= n. \qquad (3.19)$$

Thus, from Lemma 3.1 and (3.19), the intersection of the row spaces of W_p and W_f yields a valid state sequence. $\square$

There are several ways to compute the above intersection. One method is to use a QR decomposition of the matrix $\begin{bmatrix} W_p \\ W_f \end{bmatrix}$, followed by a singular value decomposition. Since the intersection can be calculated in any basis, the estimated state sequence $\hat{X}_i$ differs from the actual states X_i to within a similarity transformation. Once the estimates $\hat{X}_i$ of the state sequence X_i are computed, the system matrices can be computed by solving the least squares problems

$$\underset{A,B}{\text{argmin}} \left\| \hat{X}_{i+1} - \begin{bmatrix} A & B \end{bmatrix} \begin{bmatrix} \hat{X}_i \\ U_{i|i} \end{bmatrix} \right\|_F, \quad (3.20)$$

$$\underset{\Theta_{CG},D}{\text{argmin}} \left\| Y_{i|i} - \begin{bmatrix} \Theta_{CG} & D \end{bmatrix} \begin{bmatrix} f_{CG}(\hat{X}_i) \\ U_{i|i} \end{bmatrix} \right\|_F, \quad (3.21)$$

where $f_{CG} \colon \mathbb{R}^n \to \mathbb{R}^{\hat{s}}$ are basis functions, and $\Theta_{CG} f_{CG}(\hat{X}_i) \approx CX_i + GH_{i|i}$.

When additional noise terms are present in (3.1) and (3.2) the oblique projection method described in (Van Overschee and De Moor, 1996) is used to estimate the states. The calculation of the state space matrices remain the same as (3.20)-(3.21).

3.1.3. Hammerstein-Wiener Extension Identification for H-W systems is a straightforward extension of the Wiener identification problem described in the previous section. Consider the nonlinear discrete-time system

$$x_{k+1} = Ax_k + \mathcal{F}(u_k) + w_k, \qquad (3.22)$$

$$y_k = Cx_k + Gh(x_k) + \mathcal{G}(u_k) + v_k, \quad (3.23)$$

where $\mathcal{F} \colon \mathbb{R}^m \to \mathbb{R}^n$ and $\mathcal{G} \colon \mathbb{R}^m \to \mathbb{R}^l$. By writing $\mathcal{F}$ and $\mathcal{G}$ in terms of a set of basis functions $f \colon \mathbb{R}^m \to \mathbb{R}^s$ (Palanthandalam-Madapusi *et al.*, 2004; Lacy and Bernstein, 2001), the system can be rewritten as

$$x_{k+1} = Ax_k + Bf(u_k) + w_k, \qquad (3.24)$$

$$y_k = Cx_k + Gh(x_k) + Df(u_k) + v_k, \quad (3.25)$$

where the matrices B and D contain the coefficients of the basis function expansion. Thus, by using a basis function expansion for the input nonlinearity, the identification problem is reduced to a Wiener identification problem with generalized inputs. For details of the above procedure see (Palanthandalam-Madapusi *et al.*, 2004).

4. SUBSPACE IDENTIFICATION WITH MISSING DATA

This section considers the case in which some data points are unavailable. Let q be a time step for which a measurement of u_q or y_q is unavailable. Then we define the output block Hankel matrix

$$Y_{0|2i-1} \triangleq$$

$$\begin{bmatrix} y_0 & \cdots & y_{q-2i+1} & y_{q+1} & \cdots & y_{j-1} \\ \vdots & \ddots & \vdots & \vdots & \ddots & \vdots \\ y_{i-1} & \cdots & y_{q-i-1} & y_{q+i-1} & \cdots & y_{i+j-2} \\ y_i & \cdots & y_{q-i} & y_{q+i} & \cdots & y_{i+j-1} \\ \vdots & \ddots & \vdots & \vdots & \ddots & \vdots \\ y_{2i-1} & \cdots & y_{q-1} & y_{q+2i-1} & \cdots & y_{2i+j-2} \end{bmatrix}$$

$$(4.1)$$

$$= \begin{bmatrix} Y_{0|i-1} \\ Y_{i|2i-1} \end{bmatrix} = \begin{bmatrix} Y_p \\ Y_f \end{bmatrix}. \qquad (4.2)$$

Note that $Y_{0|2i-1}$ has the same form as the output block Hankel matrices defined in (Van Overschee and De Moor, 1996) and section 3.1, except that all the columns of the original $Y_{0|2i-1}$ containing y_q are omitted. When several data points are missing, the block Hankel matrix is constructed similarly by omitting all columns that contain the time steps corresponding to the missing data. Furthermore,

$$Y_{0|2i-1} = \begin{bmatrix} Y_{0|i} \\ Y_{i+1|2i-1} \end{bmatrix} = \begin{bmatrix} Y_p^+ \\ Y_f^- \end{bmatrix}. \qquad (4.3)$$

The input block Hankel matrices $U_{0|2i-1}$, U_p, U_f, U_p^+ and U_f^- are defined analogous to (4.1)-(4.3) with y replaced by u. Finally, the state sequences X_0 and X_i are defined as

$$X_0 \triangleq \begin{bmatrix} x_0 & \cdots & x_{q-2i+1} & x_{q+1} & \cdots & x_{i+j-1} \end{bmatrix},$$
$$X_i \triangleq \begin{bmatrix} x_i & \cdots & x_{q-i} & x_{q+i} & \cdots & x_{i+j-1} \end{bmatrix}. \quad (4.4)$$

These state sequences have a gap of $2i - 1$ time steps when one data point (u_q or y_q) is missing. X_0 has states missing from time steps $q - 2i + 2$ through q, while X_i has states missing from time step $q - i + 1$ through $q + i - 1$.

With these modified definitions of block Hankel matrices, it can be shown that, in the deterministic case, the state sequence estimated by the procedures described in (Van Overschee and De Moor, 1996) is indeed X_i defined as (4.4). Furthermore, when the noise terms are present, the procedures in (Van Overschee and De Moor, 1996) yield optimal estimates of X_i. The above modification is valid for the H-W identification procedure described in section 3.1 as well.

5. IDENTIFICATION OF PERIODICALLY SWITCHING MODELS

To identify periodically switching models, consider

$$x_{k+1} = A_k x_k + B_k u_k + w_k, \quad (5.1)$$
$$y_k = C_k x_k + D_k u_k + v_k, \quad (5.2)$$

where the period is p and switching occurs at time steps $\alpha p + r_1, \alpha p + r_2, \cdots, \alpha p + r_\beta$. Here α is any integer, β is the number of switching models and $r_1 < r_2 < \cdots < r_\beta$ are the offset switching times. Hence, for all k, $A_k = A_{k+p}$, and, for $t = 1, \ldots, \beta$,

$$A_{\alpha p + r_{t-1} + 1} = A_{\alpha p + r_{t-1} + 2} = \cdots = A_{\alpha p + r_t},$$

and similarly for B_k, C_k, D_k.

To identify the tth set of state-space matrices, the data points corresponding to all of the other sets of matrices are regarded as missing data points as in section 4. This procedure is applicable to the three H-W identification algorithms described before, but requires prior knowledge of the offset switching times r_i, and requires that

$$r_t - r_{t-1} \geq 2i, \quad t = 1, \ldots, \beta. \quad (5.3)$$

6. IDENTIFICATION FOR MAGNETOMETER DATA

The ACE IMF and solar wind data are used as inputs to the model, while the ground-based magnetometer data are used as outputs of the model. Knowledge of the physics and previous experience (Palanthandalam-Madapusi *et al.*, 2005) suggests that a combination of the B_z and B_y components is desirable for the inputs to the model, where B_z and B_y are the z and y components of the magnitude of the IMF, respectively. On testing several combinations of these two components, it is found that $B_t V_x \sin^4(\theta/2)$ works best, where

$B_t \triangleq \sqrt{B_y^2 + B_z^2}$, $\theta \triangleq a\cos B_z/B_t$, and V_x is the x-component of the velocity of the IMF. Similar combinations of terms have previously been considered (Akasofu, 2000). Additional linearly entering inputs include the density of plasma (solar wind), B_t, B_z, and B_y.

Since the flow pattern of the inonospheric currents is in a Sun-fixed coordinate system with the magnetometer station rotating within it, the system has a one-day periodicity. Periodically switching H-W models are used to capture this one-day periodicity and model the different dynamics governing the nightside and dayside of the magnetospheric system.

Switching between two, three, and four sets of state-space matrices within a one-day period are considered. The offset switching times are chosen such that an equal amount of time is spent in each regime. Thus, if two switching models are present in a day, switching occurs every 12 hours.

7. IDENTIFICATION RESULTS

For illustration, data for the month of January, 1999 measured by the ground-based magnetometer at Thule, Greenland, is used. The first 15 days' data are used for identification, while the next 16 days are used for validation. The output of the identified periodically switching H-W model using the first method is shown in Figure 2. In this model, switching between three sets of state-space matrices occurs at regular time intervals of 8 hours each. Data to the left of the black vertical line are used for identification, while the identified model is used to predict the data to the right of the vertical line. When using real-time data, prediction of only one hour is possible, however prediction for 16 days is possible in the above example since the inputs for the entire period are available. Figure 3 shows the output of the periodically switching H-W model identified using the second method. Again, switching occurs every 8 hours. Finally, the output of the periodically switching H-W model identified using the third method is shown in figure 4.

The prediction efficiencies of the three periodically switching H-W models are calculated as $PE = 1 - \sum_k (y_k - \hat{y}_k)^2 / \sigma_y^2$ (Weigel *et al.*, 2003), where σ_y^2 is the variance of the measured output y. From Table 1, the prediction efficiency for periodically switching H-W model based on the first method is seen to be better than the efficiencies for the other two methods for both the amplitude B and the fluctuation dB/dt of the magnetic field. These prediction efficiencies compare favorably to the prediction efficiencies of the neural network model in (Weigel *et al.*, 2003).

Table 1. <u>Prediction efficiencies</u>

	Method 1	Method 2	Method 3
PE for B	0.7951	0.5006	0.4958
PE for dB/dt	0.7389	0.5946	0.3114

8. CONCLUSION

Two existing Hammerstein-Wiener identification algorithms and a novel Hammerstein-Wiener identification algorithm were considered for application to the magnetospheric system. A modified subspace algorithm that allows missing data points was described and used for identifying periodically switching models. To capture the periodically time-varying nature of the system, periodically switching Hammerstein-Wiener models were then identified using the three Hammerstein-Wiener identification methods. The inputs to the models were measurements from the ACE satellite, while the outputs of the model were ground-based magnetometer readings. The prediction efficiencies of the three methods were compared. Future work will focus on other lower-latitude magnetometers and identification based on richer model structures.

9. ACKNOWLEDGEMENT

REFERENCES

Akasofu, S.-I. (2000). Predicting geomagnetic storms as a space weather project. In: *Space Weather Study Using Multipoint Techniques* (Ling-Hsiao Lyu, Ed.). Vol. 12 of *Proceedings of COSPAR*. pp. 3–20.

Bernstein, D. S. (2005). *Matrix Mathematics: Theory, Facts, and Formulas with Application to Linear Systems Theory*. Princeton University Press.

Goethals, I., K. Pelckmans, J.A.K. Suykens and B. De Moor (2004). Subspace identification of hammerstein systems using least squares support vector machines. preprint.

Hench, J. J. (1995). A technique for the identification of linear periodic state-space models. *Int. J. Cont.* **62**(2), 289–301.

Lacy, S. L. and D. S. Bernstein (2001). Subspace Identification for Nonlinear Systems That Are Linear in Unmeasured States. In: *Proc. Conf. Dec. Contr.*. Orlando, Florida. pp. 3518–3523.

Palanthandalam-Madapusi, H., A. J. Ridley and D. S. Bernstein (2005). Identification and prediction of ionospheric dynamics using a hammerstein-wiener model. In: *Proc. Amer. Contr. Conf.*. Portland, OR. pp. 5052–5057.

Palanthandalam-Madapusi, H., J. B. Hoagg and D. S. Bernstein (2004). Basis-function optimization for subspace-based nonlinear identification of systems with measured-input nonlinearities. In: *Proc. Amer. Contr. Conf.*. Boston, MA. pp. 4788–4793.

Powell, K.G., P.L. Roe, T.J. Linde, T.I. Gombosi and D.L. De Zeeuw (1999). A solution-adaptive upwind scheme for ideal magnetohydrodynamics. *J. Comp. Phys.* **154**, 284.

Van Overschee, P. and B. De Moor (1996). *Subspace Identification for Linear Systems: Theory, Implementation, Applications*. Kluwer.

Verhaegen, M. and X. Yu (1995). A class of subspace model identification algorithms to identify periodically and arbitrarily time-varying systems. *Automatica* **31**(2), 201–216.

Weigel, R. S., A. J. Klimas and D. Vassiliadis (2003). Solar wind coupling to and predictability of ground magnetic fields and their time derivatives. *J. of Geophysical Research* **108**(A7), SMP 16–1 – SMP 16–14.
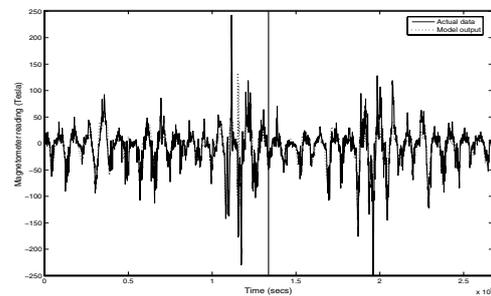
Fig. 2. Measured and predicted data of the Thule magnetometer using the first identified periodically switching H-W model.
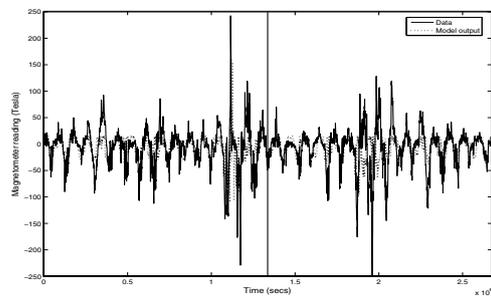
Fig. 3. Measured and predicted data of the Thule magnetometer using the second identified periodically switching H-W model.
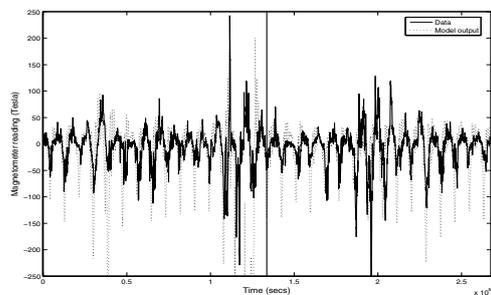
Fig. 4. Measured and predicted data of the Thule magnetometer using the third identified periodically switching H-W model.